Geophysical Journal International

Geophys. J. Int. (2011) **184,** 1397–1414 doi: 10.1111/j.1365-246X.2010.04923.x

The one-bit noise correlation: a theory based on the concepts of coherent and incoherent noise

Paul Cupillard, Laurent Stehly* and Barbara Romanowicz

Seismological Laboratory, University of California, Berkeley, CA 94720, *USA. E-mail: paulcup@ipgp.jussieu.fr*

Accepted 2010 December 13. Received 2010 December 5; in original form 2010 July 31

SUMMARY

Waveforms emerging from correlations of long seismic noise records are extensively used to investigate the crustal and upper-mantle structure of the Earth. To remove the non-stationary events that inevitably lie in seismic records, the so-called one-bit normalization is commonly applied to the noise data. This processing consists of replacing each sample of a record by its sign. Although it is a strong non-linear operation, it preserves the phase of the signal emerging from correlation. Some recent studies show that information can also be extracted from the amplitude of such correlations. In this paper, we develop a theory to understand these non-intuitive results. A statistical approach is used to get an expression of the one-bit noise correlation. This expression involves the standard deviations of coherent and incoherent noise. These two kinds of noise are precisely defined, and explicit expressions of their standard deviations are given in the case of a uniform distribution of noise sources generating surface waves on a layered half-space. In this case, we show that the one-bit noise correlation has the same phase and relative amplitude as the raw noise correlation. This is true in both elastic and anelastic media. Numerical simulations are performed to support our theory.

Key words: Interferometry; Seismic attenuation; Theoretical seismology; Wave propagation.

1 INTRODUCTION

Seismic noise correlations are now widely used to get information about the structure of the Earth. Prior to correlation, different processing steps have to be applied to the noise records. One of the most common processings is the one-bit normalization. It consists of retaining only the sign (+1 or −1) of each sample in the records. It was first introduced in communication theory. Bond & Cahn (1958) demonstrated the possibility of transmitting a continuous signal over a discrete channel by preserving the occurrence of the zero crossings only. Later, Voelcker (1966a,b) and Voelcker & Requicha (1973) extended this result to get modulation procedures for representing signals in terms of real and complex zeros. In seismology, Campillo & Paul (2003) used the one-bit normalization to process seismic coda. In this case, it enhances multiple scattering and thus improves the signal-to-noise ratio of coda correlations (Larose *et al.* 2004). In the context of long noise records, the one-bit normalization enables to remove non-stationary signals like earthquakes or spikes. For examples of applications of this technique, one can refer to Shapiro & Campillo (2004), Shapiro *et al.* (2005), Larose *et al.* (2007) and Yao & van der Hilst (2009). More sophisticated temporal normalizations can be found in Bensen *et al.* (2007) and Brooks & Gerstoft (2009).

The most common way to image the Earth interior from ambient seismic noise consists in evaluating dispersion curves of surface waves emerging from noise correlations. Since most of the noise energy ranges from 5 to 20 s period, the obtained images provide information on crustal and upper-mantle structure (e.g. Shapiro *et al.* 2005; Yao *et al.* 2006; Cho *et al.* 2007; Lin *et al.* 2007; Yang *et al.* 2007; Bensen *et al.* 2008; Lin *et al.* 2008; Yao *et al.* 2008; Stehly *et al.* 2009). Several studies also attempted to use the amplitude of noise correlations to investigate the origin of the seismic noise (Stehly *et al.* 2006; Pedersen *et al.* 2007; Yang & Ritzwoller 2008) and retrieve the attenuation of the Earth (Matzel 2008; Prieto *et al.* 2009). It is extremely interesting to note that all these works apply one-bit normalization or other strong non-linear operations to the noise records. In spite of such operations, information contained in both phase and amplitude of the correlations seems to be preserved. Understanding this non-intuitive phenomenon is the primary motivation for this work.

Voelcker (1966a) showed that zeros are fundamental informational attributes of signals. Therefore, it is not very surprising to retrieve some interesting information in one-bit noise correlations. Nevertheless, because of the lack of a theory, it is not clear so far what is effectively

*Now at: Géoazur, Université de Nice - Sophia Antipolis, 06108 Nice Cedex 02, France.

recovered. In this paper, a theoretical development is proposed to explain the full waveform (phase and amplitude) of the one-bit noise correlation. First, we follow Snieder (2004) to get an expression of the raw noise correlation. Using this expression and a statistical approach similar to Derode *et al.* (1999) and Larose *et al.* (2008), we introduce the concepts of coherent and incoherent noise. These two kinds of noise are Gaussian and their variances can be evaluated using the central limit theorem. Then, we look at the one-bit noise correlation: we apply basic laws of probability to the samples of one-bit noise records and we obtain a formula for the correlation. This formula involves the standard deviations of both coherent and incoherent noise. In this work, we provide explicit expressions for these standard deviations in the context of surface waves propagating in a layered medium. Extension to body waves and full 3-D cases is discussed at the end of the paper. Both elastic and anelastic cases are investigated.

2 THE RAW NOISE CORRELATION

2.1 General expression of the raw noise correlation

Consider two stations A and B that are separated by a distance Δ. These stations respectively record signals $A(t)$ and $B(t)$ due to random noise sources acting in the medium. We denote by $A_p(t)$, $B_p(t)$ the signal received in A, B, respectively, from a single point-source P. The correlation between $A(t)$ and $B(t)$ can thus be written as

$$C_{AB}(t) = \sum_{p,\,p'} \int A_p(\tau) B_{p'}(t+\tau) \mathrm{d}\tau. \tag{1}$$

We assume that the signals produced by two distinct sources are uncorrelated. Therefore, the cross terms $p \neq p'$ in the double sum $\sum_{p,p'}$ vanish and expression (1) can be reduced to

$$C_{AB}(t) = \sum_{p} C^{p}_{AB}(t), \tag{2}$$

with

$$C^{p}_{AB}(t) = \int A_p(\tau) B_p(t+\tau) \mathrm{d}\tau. \tag{3}$$

In the following, the sources and receivers are placed on the surface of a laterally homogeneous half-space (the elastic parameters of the medium only depend on the depth z). For the sake of simplicity, we work with fundamental mode surface waves, but overtones could be included by introducing a summation, as done by Snieder (2004), Halliday & Curtis (2008) or Kimman & Trampert (2010). Moreover, we consider vertical displacements only, but the whole theory developed in this paper could be easily extended to all components of the Green's tensor. In the frequency domain, the vertical-vertical component of the fundamental mode surface wave Green's tensor between two points U and V is given by (Aki & Richards 2002)

$$G_{UV}(\omega) = \frac{\exp\left[-\mathrm{i}\left(k\, d_{UV} + \frac{\pi}{4}\right)\right]}{\sqrt{\frac{\pi}{2}\, k\, d_{UV}}}, \tag{4}$$

where ω is the angular frequency, $k(\omega)$ is the wavenumber and d_{UV} is the horizontal distance between U and V. Using eq. (4) and denoting by $|S_p(\omega)|^2$ the power spectral density of source P, the Fourier transform of cross-correlation (3) becomes

$$C^{p}_{AB}(\omega) = \frac{2}{\pi} |S_p(\omega)|^2 \frac{\exp\left[\mathrm{i}\, k\left(d_{AP} - d_{BP}\right)\right]}{k\sqrt{d_{AP}\, d_{BP}}}. \tag{5}$$

It follows that

$$C_{AB}(\omega) = \frac{2}{\pi} \sum_{p} |S_p(\omega)|^2 \frac{\exp\left[\mathrm{i}\, k\left(d_{AP} - d_{BP}\right)\right]}{k\sqrt{d_{AP}\, d_{BP}}}. \tag{6}$$

Replacing the summation over discrete sources by a surface integration (the variables with index p become functions of the source location $\boldsymbol{r}$), we obtain

$$C_{AB}(\omega) = \frac{2}{\pi} \iint |S(\boldsymbol{r};\omega)|^2 \frac{\exp\left[\mathrm{i}\, k\left(d_A(\boldsymbol{r}) - d_B(\boldsymbol{r})\right)\right]}{k\sqrt{d_A(\boldsymbol{r})\, d_B(\boldsymbol{r})}} \mathrm{d}\boldsymbol{r}. \tag{7}$$

2.2 The raw noise correlation in the case of a uniform distribution of sources

When $|S(\boldsymbol{r};\omega)|^2$ is a smooth function of $\boldsymbol{r}$, the integral in eq. (7) can be evaluated using the stationary phase approximation (Snieder, 2004). Let us use this approximation in a Cartesian coordinate system. We position receiver A at the origin and receiver B on the positive x-axis. Then

$$\begin{aligned} C_{AB}(\omega) = {} & \frac{2}{\mathrm{i}k} \frac{\exp\left[\mathrm{i}\left(k\Delta + \frac{\pi}{4}\right)\right]}{\sqrt{\frac{\pi}{2} k\Delta}} \int_{\Delta}^{\infty} |S(x, y=0;\omega)|^2 \mathrm{d}x \\ & - \frac{2}{\mathrm{i}k} \frac{\exp\left[-\mathrm{i}\left(k\Delta + \frac{\pi}{4}\right)\right]}{\sqrt{\frac{\pi}{2} k\Delta}} \int_{-\infty}^{0} |S(x, y=0;\omega)|^2 \mathrm{d}x. \end{aligned} \tag{8}$$

This result shows that the Green's function (GF) between A and B can emerge from the correlation of random noise records. The first term on the right-hand side contains the acausal GF and arises because of the noise sources at $x > \Delta$. The second term contains the causal GF and arises because of the sources at $x < 0$. This result is not new. It was first demonstrated by Lobkis & Weaver (2001) using the assumption of equipartitioning of the Earth's normal modes. Other proofs followed, invoking the fluctuation-dissipation theorem (van Tiggelen 2003), an analogy with time-reversal experiments (Derode *et al.* 2003), the reciprocity theorem (Wapenaar 2004) or the stationary-phase approximation (Snieder 2004).

Denoting by $v(\omega)$ the phase velocity of the fundamental mode Rayleigh wave and considering a uniform distribution of noise sources such that $|S(x, y = 0;\omega)|^2 = |S(\omega)|^2$, eq. (8) becomes

$$C_{AB}(\omega) = 2D\frac{v(\omega)|S(\omega)|^2}{\mathrm{i}\omega}\left\{\frac{\exp\left[\mathrm{i}\left(k\Delta+\frac{\pi}{4}\right)\right]}{\sqrt{\frac{\pi}{2}k\Delta}} - \frac{\exp\left[-\mathrm{i}\left(k\Delta+\frac{\pi}{4}\right)\right]}{\sqrt{\frac{\pi}{2}k\Delta}}\right\}. \tag{9}$$

We limit the integration over x to a range bounded by a finite distance $D \gg \Delta$. This is to prevent this integration to diverge. In practice, there is no problem of divergence because of intrinsic attenuation. We study this case in Section 5. Eq. (9) shows that one has to differentiate the correlation in time to get the GF. Not only the waveform but also the amplitude decay of the GF with distance Δ is retrieved by the correlation.

Fig. 1 confirms the theory. This figure shows results from a numerical experiment similar to those carried out by Cupillard & Capdeville (2010). The experiment consists in computing synthetic noise recordings in a spherical earth using a normal mode summation technique (e.g. Woodhouse & Girnius 1982). 300 sources are randomly positioned on the surface of the Earth. Each source generates a 24-hr random signal filtered between 66 and 200 s. An array of 12 receivers ($n = 0$, ..., 11) records the wavefield produced by the noise sources. The correlations between the vertical displacement at station 0 and the vertical displacement at the other stations are performed. The Earth model is PREM (Dziewonski & Anderson 1981). The configuration of the experiment is shown in Fig. 1(a). It is repeated 5120 times (64 processors perform it 80 times each) and all the obtained correlations are then stacked. You can refer to Cupillard & Capdeville (2010) for more details. Fig. 1(b) compares the time-derivative of the correlation between stations 0 and 6 with the corresponding fundamental mode GF. As predicted by the theory, the two curves match very well. We also plot the comparison between the amplitude decay of the correlation along the array and the amplitude decay of the GF. Again, the curves match very well, which confirms the theory.

3 COHERENT AND INCOHERENT NOISE

3.1 Definition

From a statistical point of view, cross-correlation (3) can be viewed as an ensemble average over time τ. Thus we can write

$$C^p_{AB}(t) = \sigma_{A_p}\sigma_{B_p}\,\rho^p_{AB}(t), \tag{10}$$

where σ_{A_p}, σ_{B_p} are the standard deviations of the stationary signals $A_p(\tau)$, $B_p(\tau)$, respectively, and $\rho^p_{AB}(t)$ is the correlation coefficient between $A_p(\tau)$ and $B_p(t+\tau)$. The standard deviation σ_{A_p}, σ_{B_p} is the square-root of the energy arriving in A, B, respectively, from a point-source P, so

$$\sigma_{A_p} = \frac{1}{\sqrt{d_{AP}}} \tag{11}$$

and

$$\sigma_{B_p} = \frac{1}{\sqrt{d_{BP}}}. \tag{12}$$

Using the inverse Fourier transform of eq. (5) we find the expression of ρ^p_{AB}.

$$\rho^p_{AB}(t) = \frac{2}{\pi}\int \frac{|S_p(\omega)|^2}{k}\exp\left[\mathrm{i}\omega\left(t - \frac{d_{BP}-d_{AP}}{v(\omega)}\right)\right]\mathrm{d}\omega. \tag{13}$$

As $\sigma^2_{A_p}$ and $\sigma^2_{B_p}$ are both energies from P, the power spectral density $|S_p(\omega)|^2$ should appear in their definitions. Nevertheless, it is possible and much more practical to put this common factor in the definition of ρ^p_{AB}. We now substitute eq. (10) into eq. (2) and replace the summation $\sum_p$ by a surface integration. This gives us

$$C_{AB}(t) = \iint \sigma_A(\boldsymbol{r})\sigma_B(\boldsymbol{r})\rho_{AB}(\boldsymbol{r};t)\,\mathrm{d}\boldsymbol{r}, \tag{14}$$

with

$$\sigma_A(\boldsymbol{r}) = \frac{1}{\sqrt{d_A(\boldsymbol{r})}}, \tag{15}$$

$$\sigma_B(\boldsymbol{r}) = \frac{1}{\sqrt{d_B(\boldsymbol{r})}}, \tag{16}$$

$$\rho_{AB}(\boldsymbol{r};t) = \frac{2}{\pi}\int \frac{|S(\boldsymbol{r};\omega)|^2}{k}\exp\left[\mathrm{i}\omega\left(t - \frac{d_B(\boldsymbol{r})-d_A(\boldsymbol{r})}{v(\omega)}\right)\right]\mathrm{d}\omega. \tag{17}$$

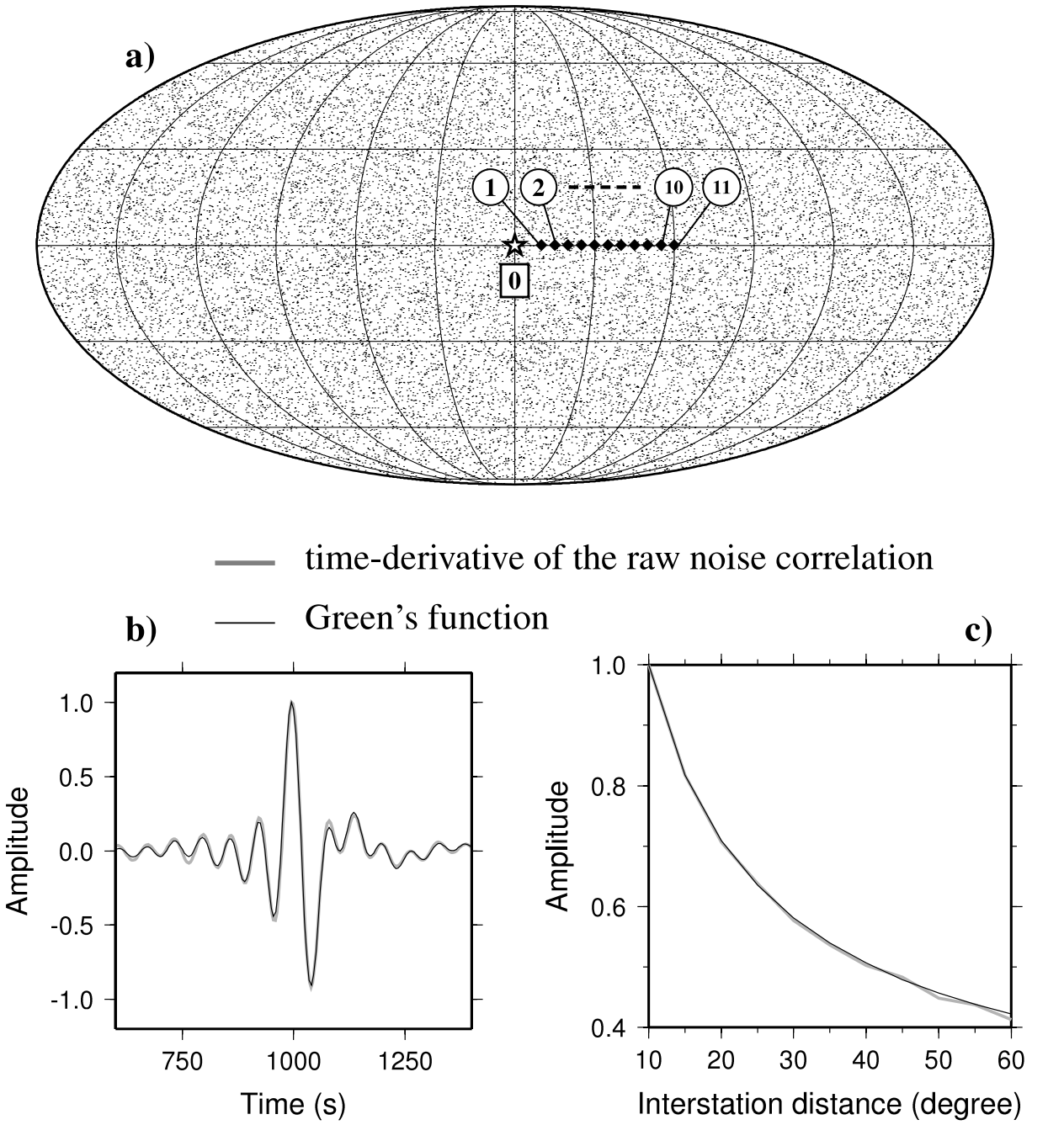

Figure 1. Source and receiver configuration of the simulation (a). Tiny pixels indicate the location of 24 000 noise sources generated by a single processor. All the sources are on the surface of the Earth. Diamonds represent 11 receivers ($n = 1, ..., 11$). Two consecutive receivers are separated by 5°. The synthetic noise record from each station is correlated with the noise recorded at receiver 0 (white star). The distance between stations 0 and 1 is 10°. We plot the time-derivative of the correlation between stations 0 and 6 and the corresponding fundamental mode Rayleigh wave GF (b). We also compare the amplitude decay of the correlation with the amplitude decay of the GF (c). We see that the correlation fits both waveform and relative amplitude of the GF.

Taking a uniform distribution of noise sources into account, we easily demonstrate (Appendix A) that

$$C^2_{AB}(t) = \iint \sigma^2_A(\boldsymbol{r})\rho_{AB}(\boldsymbol{r};t)\,\mathrm{d}\boldsymbol{r} \iint \sigma^2_B(\boldsymbol{r})\rho_{AB}(\boldsymbol{r};t)\,\mathrm{d}\boldsymbol{r}. \tag{18}$$

This last expression shows that the instantaneous energy of the correlation is the product of the two functions

$$\Psi_A(t) = \iint \sigma^2_A(\boldsymbol{r})\rho_{AB}(\boldsymbol{r};t)\,\mathrm{d}\boldsymbol{r} \tag{19}$$

and

$$\Psi_B(t) = \iint \sigma^2_B(\boldsymbol{r})\rho_{AB}(\boldsymbol{r};t)\,\mathrm{d}\boldsymbol{r}. \tag{20}$$

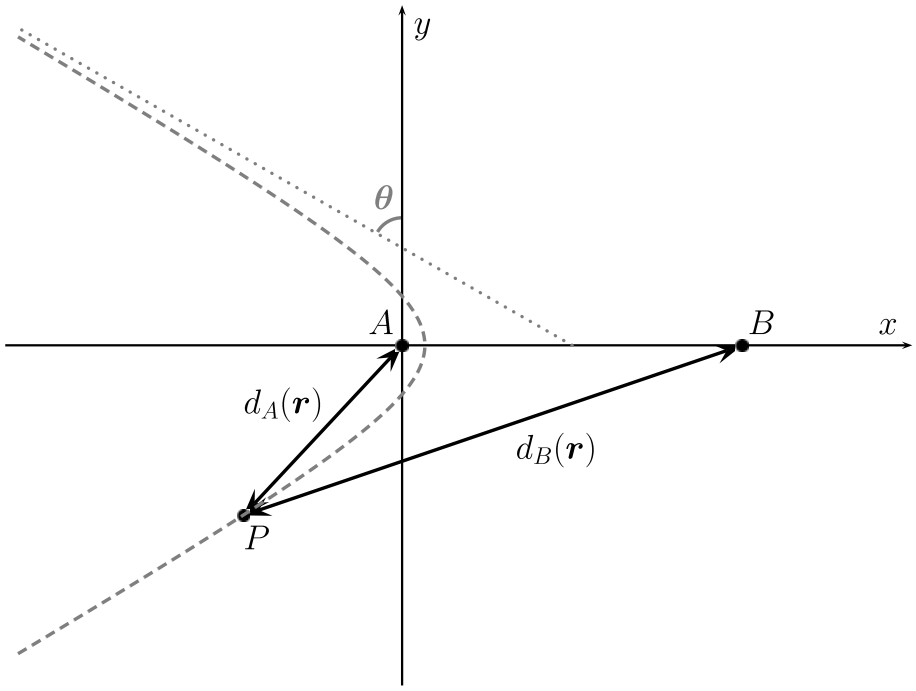

Figure 2. The two coordinate systems used in our derivation. We first consider a simple Cartesian system (x, y). Receivers A and B are positioned in $(0, 0)$ and $(0, \Delta)$, respectively. The quantity $d_A(\boldsymbol{r}) - d_B(\boldsymbol{r})$ is involved in our derivation. This quantity is constant over a hyperbola so we introduce the coordinates (θ, ϕ) to work in a more convenient way. θ is the angle between the asymptote of a given hyperbola and the y-axis. ϕ the curvilinear coordinate along each hyperbola.

Let us study $\Psi_A(t)$ and $\Psi_B(t)$. Without changing our notations, we replace all the complex time-variables by their respective real part. Eq. (18) is still valid in this case and the correlation coefficient becomes

$$\rho_{AB}(\boldsymbol{r};t) = \frac{2}{\pi}\int \frac{|S(\boldsymbol{r};\omega)|^2}{k}\cos\left[\omega\left(t - \frac{d_B(\boldsymbol{r}) - d_A(\boldsymbol{r})}{v(\omega)}\right)\right]\mathrm{d}\omega. \tag{21}$$

The value of $d_B(\boldsymbol{r}) - d_A(\boldsymbol{r})$ is constant over a hyperbola. Each hyperbola is characterized by θ which is the angle between its asymptotes and the y-axis (Fig. 2). We denote by ϕ the curvilinear coordinate along each hyperbola. Following Roux *et al.* (2005) we make the change of variables

$$\begin{cases} x = \dfrac{\Delta}{2}\sin\theta\cosh\phi + \dfrac{\Delta}{2} \\ y = \dfrac{\Delta}{2}\cos\theta\sinh\phi \end{cases} \quad \text{with} \begin{cases} \theta \in \left[-\frac{\pi}{2}, \frac{\pi}{2}\right] \\ \phi \in \mathbb{R}. \end{cases} \tag{22}$$

It follows

$$d_A(\boldsymbol{r}) = \frac{\Delta}{2}(\cosh\phi + \sin\theta), \tag{23}$$

$$d_B(\boldsymbol{r}) = \frac{\Delta}{2}(\cosh\phi - \sin\theta) \tag{24}$$

and

$$d_B(\boldsymbol{r}) - d_A(\boldsymbol{r}) = -\Delta\sin\theta. \tag{25}$$

We neglect the frequency-dependence of the phase velocity $[v(\omega) = v]$ and we use the fact that the distribution of noise sources is uniform so we can rewrite (21) as a function of θ.

$$\rho_{AB}(\theta;t) = \frac{2v}{\pi}\int \frac{|S(\omega)|^2}{\omega}\cos\left[\omega\left(t + \frac{\Delta\sin\theta}{v}\right)\right]\mathrm{d}\omega. \tag{26}$$

To perform the integration over ω, we need to choose an amplitude spectrum $|S(\omega)|$. For the sake of simplicity, we consider a boxcar function $H(\omega_0 + \frac{\Delta\omega}{2}) - H(\omega_0 - \frac{\Delta\omega}{2})$, where H is the Heaviside step function. We obtain

$$\rho_{AB}(\theta;t) = \frac{2v}{\pi}\left\{\mathrm{ci}\left[\left(\omega_0 + \frac{\Delta\omega}{2}\right)\left(t + \frac{\Delta\sin\theta}{v}\right)\right] - \mathrm{ci}\left[\left(\omega_0 - \frac{\Delta\omega}{2}\right)\left(t + \frac{\Delta\sin\theta}{v}\right)\right]\right\}, \tag{27}$$

where ci is the cosine-integral special function (Appendix B). This function is defined in the positive real number space $\mathbb{R}^{+*}$ but we can extend it to the set of negative arguments by posing $\mathrm{ci}(u) = \mathrm{ci}(-u)\ \forall u \in \mathbb{R}^{-*}$. Moreover, ci is not defined at $u = 0$ but the function in braces in eq. (27) has a finite limit when $t \to -\frac{\Delta\sin\theta}{v}$ so we can define it at 0 (Appendix B). Let us assume that the boxcar width $\Delta\omega$ is very large.

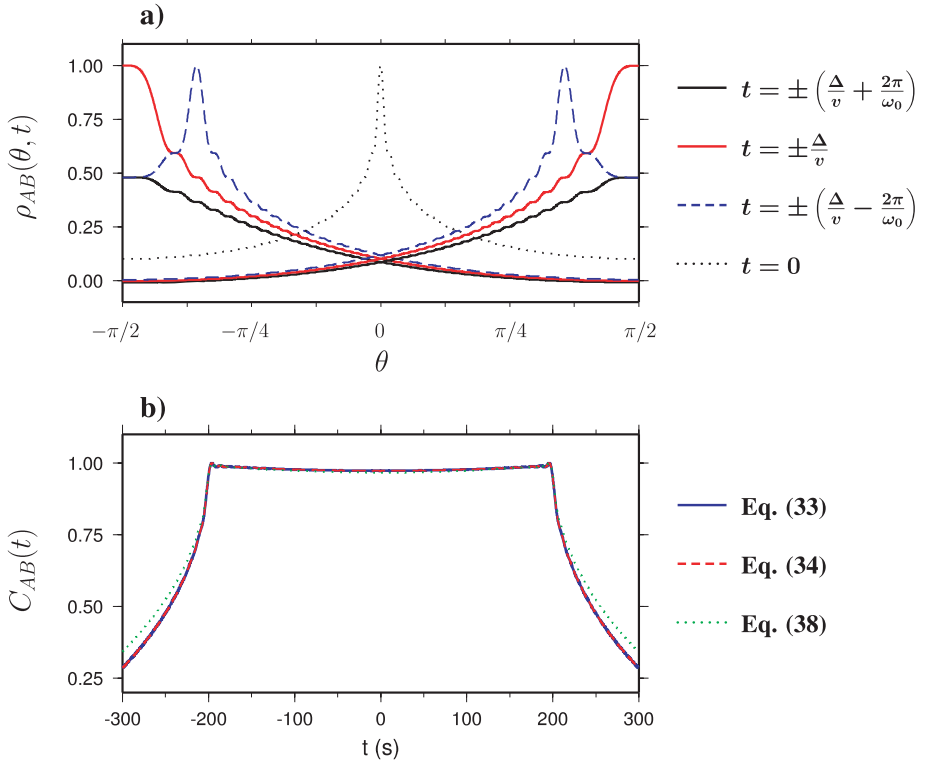

Figure 3. ρ_{AB} as a function of θ for four different values of t in the case of a large $\Delta\omega = 1.99\,\omega_0$ (a). The four curves are positive for all θ. We also plot the correlation $C_{AB}(t)$ using three different equations (b). The exact solution (eq. 33) is in blue, the solution involving the coherent noise (eq. 34) is in dashed red and the solution given by the stationary phase approximation (eq. 38) is in dotted green. For the calculation we took $f_0 = 0.05$ Hz, $v = 3\,\mathrm{km\,s^{-1}}$ and $\Delta = 10\,\lambda_0 = 600$ km.

Then $\rho_{AB}(\theta;t)$ is always positive (Fig. 3a). This means that $\Psi_A(t)$ and $\Psi_B(t)$ can be defined as sums of variances. Each variance in the sum $\Psi_A(t)$, $\Psi_B(t)$ is the energy $\sigma_A^2(\boldsymbol{r})$, $\sigma_B^2(\boldsymbol{r})$, arriving in A, B, respectively, due to a noise point-source $\boldsymbol{r}$ weighted by a positive value $\rho_{AB}(\theta;t)$. Therefore, according to the central limit theorem, there exist for each lag time t two Gaussian signals $A^t(\tau)$ and $B^t(\tau)$ with zero mean and variance $\sigma_{A^t}^2 = \Psi_A(t)$ and $\sigma_{B^t}^2 = \Psi_B(t)$, respectively, such that $A^t(\tau)$ and $B^t(t+\tau)$ are perfectly correlated and give rise to $C_{AB}(t)$. In other words,

$$C_{AB}(t) = \int A^t(\tau)B^t(t+\tau)\mathrm{d}\tau = \sigma_{A^t}\sigma_{B^t}. \tag{28}$$

We call $A^t(\tau)$ and $B^t(\tau)$ coherent noise at lag time t. We also define incoherent noise:

$$\overline{A^t}(\tau) = A(\tau) - A^t(\tau) \tag{29}$$

and

$$\overline{B^t}(\tau) = B(\tau) - B^t(\tau), \tag{30}$$

with variances $\sigma_{\overline{A^t}}^2$ and $\sigma_{\overline{B^t}}^2$. From eqs (28) to (30), it follows that

$$\int \overline{A^t}(\tau)\overline{B^t}(t+\tau)\mathrm{d}\tau + \int \overline{A^t}(\tau)B^t(t+\tau)\mathrm{d}\tau + \int A^t(\tau)\overline{B^t}(t+\tau)\mathrm{d}\tau = 0. \tag{31}$$

3.2 Comparing three different expressions of the raw noise correlation

Fig. 3(b) shows the correlation $C_{AB}(t)$ computed in three different ways.

(i) Using eqs (23), (24) and (27) and the Jacobian of the change of variable (22)

$$J = \left(\frac{\Delta}{2}\right)^2 (\cosh^2\phi - \sin^2\theta), \tag{32}$$

we can rewrite the exact solution (14) as

$$C_{AB}(t) = \frac{v\Delta}{\pi}\int_{-\frac{\pi}{2}}^{\frac{\pi}{2}}\int_0^{\phi_0}\sqrt{\cosh^2\phi - \sin^2\theta}\{\mathrm{ci}^+ - \mathrm{ci}^-\}\mathrm{d}\phi\mathrm{d}\theta, \tag{33}$$

where $\mathrm{ci}^+ = \mathrm{ci}[(\omega_0 + \frac{\Delta\omega}{2})(t + \frac{\Delta \sin\theta}{v})]$, $\mathrm{ci}^- = \mathrm{ci}[(\omega_0 - \frac{\Delta\omega}{2})(t + \frac{\Delta \sin\theta}{v})]$ and $\phi_0 \gg 1$ is a finite value we introduce to bound the integration over ϕ (such as D in eq. 9). A numerical calculation of the double integral gives the curve in blue.

(ii) Using again eqs (23), (24), (27) and (32) we can express $\Psi_A(t)$ and $\Psi_B(t)$ as a function of θ and ϕ_0. Then we can rewrite (28).

$$\begin{aligned} C_{AB}(t) &= \sigma_{A^t}\sigma_{B^t} \\ &= \sqrt{\Psi_A(t)}\sqrt{\Psi_B(t)} \\ &= \sqrt{\frac{v\Delta}{\pi}\int_{-\frac{\pi}{2}}^{\frac{\pi}{2}}(\sinh\phi_0 - \phi_0\sin\theta)\{\mathrm{ci}^+ - \mathrm{ci}^-\}\mathrm{d}\theta}\sqrt{\frac{v\Delta}{\pi}\int_{-\frac{\pi}{2}}^{\frac{\pi}{2}}(\sinh\phi_0 + \phi_0\sin\theta)\{\mathrm{ci}^+ - \mathrm{ci}^-\}\mathrm{d}\theta}. \end{aligned} \tag{34}$$

The two integrations over θ are performed numerically. We obtain the dashed red curve in Fig. 3(b). We see that this curve is indistinguishable from the blue curve, which confirms expression (18). It is actually very easy to give another proof, different from Appendix A, of this expression. Indeed, ϕ_0 is large so both $\Psi_A(t)$ and $\Psi_B(t)$ reduce to

$$\Psi_A(t) = \Psi_B(t) = \frac{v\Delta \mathrm{e}^{\phi_0}}{2\pi}\int_{-\frac{\pi}{2}}^{\frac{\pi}{2}}\{\mathrm{ci}^+ - \mathrm{ci}^-\}\mathrm{d}\theta. \tag{35}$$

Eq. (33) also reduces to

$$C_{AB}(t) = \frac{v\Delta \mathrm{e}^{\phi_0}}{2\pi}\int_{-\frac{\pi}{2}}^{\frac{\pi}{2}}\{\mathrm{ci}^+ - \mathrm{ci}^-\}\mathrm{d}\theta \tag{36}$$

so

$$C_{AB}^2(t) = \Psi_A(t)\Psi_B(t). \tag{37}$$

(iii) The expression of the correlation obtained using the stationary phase approximation is also plotted in Fig. 3(b) (dotted green). It corresponds to the real part of the inverse Fourier transform of eq. (9).

$$C_{AB}(t) = 2Dv\int_{\omega_0-\frac{\Delta\omega}{2}}^{\omega_0+\frac{\Delta\omega}{2}}\frac{1}{\omega}\left[\frac{\cos\left(\omega t + k\Delta - \frac{\pi}{4}\right)}{\sqrt{\frac{\pi}{2}k\Delta}} + \frac{\cos\left(\omega t - k\Delta + \frac{\pi}{4}\right)}{\sqrt{\frac{\pi}{2}k\Delta}}\right]\mathrm{d}\omega. \tag{38}$$

This approximate solution is good but not excellent. This is because $\Delta\omega$ is large. Very low frequencies are therefore involved and the exponential in the integrand in eq. (7) does not oscillate much.

3.3 Studying the case of narrow band sources

In practice, $\Delta\omega$ is not large; most of the ambient noise energy is concentrated between 5 and 20 s (Longuet-Higgins 1950; Friedrich *et al.* 1998; Schulte-Pelkum *et al.* 2004; Stehly *et al.* 2006; Gerstoft & Tanimoto 2007; Pedersen *et al.* 2007; Kedar *et al.* 2008; Stutzmann *et al.* 2009), so $\Delta\omega \sim \omega_0$. In this case, $\rho_{AB}(\theta;t)$ can be negative (Fig. 4a) and $\Psi_A(t)$ and $\Psi_B(t)$ as expressed in (19) and (20) are no longer sums of variances. Nevertheless, the stationary phase approximation can be used to rewrite these equations.

$$\begin{aligned} \Psi_A(t) = &\int_{\Delta}^{D+\frac{\Delta}{2}}\sigma_A^2(x, y=0)\rho_{AB}(x, y=0;t)\mathrm{d}x\left\{1 + o\left[(\Delta/D)^0\right]\right\} \\ &+ \int_{\frac{\Delta}{2}-D}^{0}\sigma_A^2(x, y=0)\rho_{AB}(x, y=0;t)\mathrm{d}x\left\{1 + o\left[(\Delta/D)^0\right]\right\} \end{aligned} \tag{39}$$

and

$$\begin{aligned} \Psi_B(t) = &\int_{\Delta}^{D+\frac{\Delta}{2}}\sigma_B^2(x, y=0)\rho_{AB}(x, y=0;t)\mathrm{d}x\left\{1 + o\left[(\Delta/D)^0\right]\right\} \\ &+ \int_{\frac{\Delta}{2}-D}^{0}\sigma_B^2(x, y=0)\rho_{AB}(x, y=0;t)\mathrm{d}x\left\{1 + o\left[(\Delta/D)^0\right]\right\}, \end{aligned} \tag{40}$$

with

$$\rho_{AB}(x, y=0;t) = v\sqrt{x(x-\Delta)}\int_{\omega_0-\frac{\Delta\omega}{2}}^{\omega_0+\frac{\Delta\omega}{2}}\frac{1}{\omega}\left[\frac{\cos\left(\omega t + k\Delta - \frac{\pi}{4}\right)}{\sqrt{\frac{\pi}{2}k\Delta}} + \frac{\cos\left(\omega t - k\Delta + \frac{\pi}{4}\right)}{\sqrt{\frac{\pi}{2}k\Delta}}\right]\mathrm{d}\omega. \tag{41}$$

These expressions are easily obtained using eqs (A5)–(A8). Eq. (41) shows that the sign of ρ_{AB} is a constant over x for a given lag time t, so we can define coherent noise $A^t(\tau)$ and $B^t(\tau)$ with variances $\sigma_{A^t}^2$ and $\sigma_{B^t}^2$, respectively, as we did in the previous paragraph. We have

$$\sigma_{A^t}^2 = \mathrm{sgn}\left[\rho_{AB}(x, y=0;t)\right]\Psi_A(t) \tag{42}$$

$$\begin{aligned} = &\int_{\Delta}^{D+\frac{\Delta}{2}}\sigma_A^2(x, y=0)|\rho_{AB}(x, y=0;t)|\mathrm{d}x\left\{1 + o\left[(\Delta/D)^0\right]\right\} \\ &+ \int_{\frac{\Delta}{2}-D}^{0}\sigma_A^2(x, y=0)|\rho_{AB}(x, y=0;t)|\mathrm{d}x\left\{1 + o\left[(\Delta/D)^0\right]\right\}, \end{aligned} \tag{43}$$

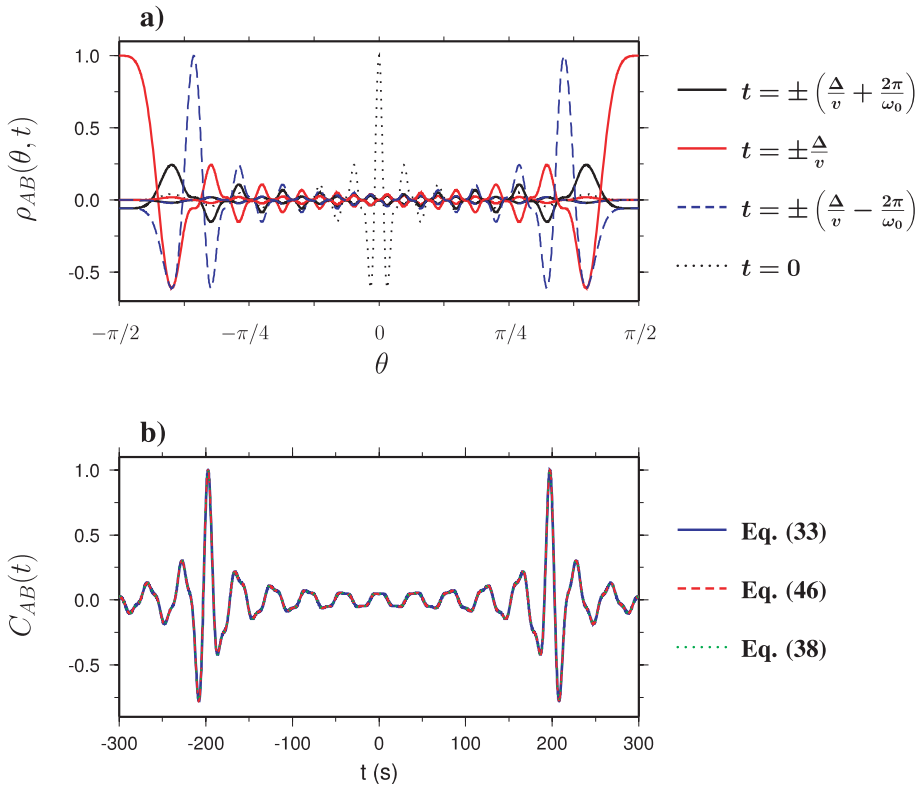

Figure 4. ρ_{AB} as a function of θ for four different values of t in the case of a small $\Delta\omega = \omega_0$ (a). Unlike the case of a large $\Delta\omega$ shown in Fig. 3, the four curves can be positive or negative depending on θ. The correlation $C_{AB}(t)$ is also plotted using three different equations (b). The exact solution (eq. 33) is in blue, the solution involving the coherent noise (eq. 46) is in dashed red and the solution given by the stationary phase approximation (eq. 38) is in dotted green. For the calculation we took $f_0 = 0.05$ Hz, $v = 3\,\mathrm{km\,s^{-1}}$ and $\Delta = 10\,\lambda_0 = 600$ km.

$$\sigma_{B^t}^2 = \mathrm{sgn}\left[\rho_{AB}(x, y=0; t)\right]\Psi_B(t) \tag{44}$$

$$= \int_{\Delta}^{D+\frac{\Delta}{2}} \sigma_B^2(x, y=0)|\rho_{AB}(x, y=0; t)|dx\left\{1 + o\left[(\Delta/D)^0\right]\right\}$$
$$+ \int_{\frac{\Delta}{2}-D}^{0} \sigma_B^2(x, y=0)|\rho_{AB}(x, y=0; t)|\mathrm{d}x\left\{1 + o\left[(\Delta/D)^0\right]\right\} \tag{45}$$

and

$$C_{AB}(t) = \int A^t(\tau)B^t(t+\tau)\mathrm{d}\tau = \mathrm{sgn}\left[\rho_{AB}(x, y=0; t)\right]\sigma_{A^t}\sigma_{B^t}. \tag{46}$$

In the last equation we see that the sign of ρ_{AB} indicates if $A^t(\tau)$ and $B^t(t+\tau)$ are perfectly correlated or perfectly anticorrelated. Of course we can also define incoherent noise.

Again, we plot $C_{AB}(t)$ using three different equations (Fig. 4b). (i) The exact solution (33) is represented in blue. (ii) The result from the stationary phase approximation (eq. 38) is the dotted green curve. We see that it perfectly fits the blue curve, meaning that the approximation is very good when $\Delta\omega = \omega_0$. (iii) The dashed red curve corresponds to eq. (46). In this last equation, σ_{A^t} and σ_{B^t} are obtained putting expression (41) in (43) and (45). This gives

$$\sigma_{A^t} = \sigma_{B^t} = \sqrt{2Dv\left|\int_{\omega_0-\frac{\Delta\omega}{2}}^{\omega_0+\frac{\Delta\omega}{2}} \frac{1}{\omega}\left[\frac{\cos\left(\omega t + k\Delta - \frac{\pi}{4}\right)}{\sqrt{\frac{\pi}{2}k\Delta}} + \frac{\cos\left(\omega t - k\Delta + \frac{\pi}{4}\right)}{\sqrt{\frac{\pi}{2}k\Delta}}\right]\mathrm{d}\omega\right|} \tag{47}$$

$$= \sqrt{|C_{AB}(t)|} \tag{48}$$

The fact that both σ_{A^t} and σ_{B^t} are equal to the square root of the correlation is not surprising. Indeed, expressions (39) and (40) have been obtained using the zeroth-order version ($o[(\Delta/D)^0]$) of eqs (A6) and (A8). In this case, both $\Psi_A(\omega)$ and $\Psi_B(\omega)$ are equal to $C_{AB}(\omega)$. This explains why the blue and the dashed red curves are identical in the figure.

4 THE ONE-BIT NOISE CORRELATION

4.1 General expression of the one-bit noise correlation

One-bit normalization consists of retaining only the sign of the raw signal by replacing all positive amplitudes with a 1 and all negative amplitudes with a −1. The one-bit noise correlation $C_{AB}^{ob}(t)$ between $A(t)$ and $B(t)$ can be written

$$C_{AB}^{ob}(t) = \int \mathrm{sgn}[A(\tau)]\,\mathrm{sgn}[B(t+\tau)]\,\mathrm{d}\tau \tag{49}$$

$$= n_1(t) - n_{-1}(t), \tag{50}$$

where $n_1(t)$ and $n_{-1}(t)$ are the number of samples for which $\mathrm{sgn}[A(\tau)] = \mathrm{sgn}[B(t+\tau)]$, and $\mathrm{sgn}[A(\tau)] \neq \mathrm{sgn}[B(t+\tau)]$, respectively.

For some samples τ, $|\overline{A^t}(\tau)| > |A^t(\tau)|$ or $|\overline{B^t}(t+\tau)| > |B^t(t+\tau)|$: at one of the two stations, the incoherent noise has a larger amplitude than the coherent noise and so controls the sign of the sample at this station. In this case, the two events $\mathrm{sgn}[A(\tau)] = \mathrm{sgn}[B(t+\tau)]$ and $\mathrm{sgn}[A(\tau)] \neq \mathrm{sgn}[B(t+\tau)]$ have the same probability. This is because of the incoherency of the random signals $\overline{A^t}(\tau)$ and $\overline{B^t}(t+\tau)$ (*cf.* eq. 31). Therefore we have $n_1(t) = n_{-1}(t)$ for this population of samples, which means that there is no contribution from this population to the value of $C_{AB}^{ob}(t)$.

For the other samples, $|\overline{A^t}(\tau)| < |A^t(\tau)|$ and $|\overline{B^t}(t+\tau)| < |B^t(t+\tau)|$: the coherent noise controls the sign of both $A(\tau)$ and $B(t+\tau)$, so $\mathrm{sgn}[A(\tau)] = \mathrm{sgn}[A^t(\tau)]$ and $\mathrm{sgn}[B(t+\tau)] = \mathrm{sgn}[B^t(t+\tau)]$. Because of the perfect correlation or anticorrelation between $A^t(\tau)$ and $B^t(t+\tau)$ (*cf.* eqs 28 and 46) we have $\mathrm{sgn}[B^t(t+\tau)] = \mathrm{sgn}[A^t(\tau)]\,\forall\tau$ (so $n_{-1}(t) = 0$) or $\mathrm{sgn}[B^t(t+\tau)] \neq \mathrm{sgn}[A^t(\tau)]\,\forall\tau$ (so $n_1(t) = 0$). Therefore, we can write

$$|C_{AB}^{ob}(t)| = n P_A^t P_B^t, \tag{51}$$

where n is the total number of samples in the correlation, P_A^t is the probability that $|A^t(\tau)| > |\overline{A^t}(\tau)|$ and P_B^t is the probability that $|B^t(\tau)| > |\overline{B^t}(\tau)|$.

Coherent and incoherent noise are both Gaussian so we are able to express P_A^t and P_B^t (Appendix C). Denoting by $\sigma_{\overline{A^t}}$ and $\sigma_{\overline{B^t}}$ the standard deviation of $\overline{A^t}(\tau)$ and $\overline{B^t}(\tau)$, respectively, we find

$$|C_{AB}^{ob}(t)| = n\left[1 - \frac{2}{\pi}\arctan\left(\frac{\sigma_{\overline{A^t}}}{\sigma_{A^t}}\right)\right]\left[1 - \frac{2}{\pi}\arctan\left(\frac{\sigma_{\overline{B^t}}}{\sigma_{B^t}}\right)\right]. \tag{52}$$

Eq. (52) is the most important result of this paper. It gives the expression of the one-bit noise correlation and shows how it is related to physical parameters. The involved physical parameters are the standard deviations of coherent and incoherent noise. More precisely, the ratio $w_{R^t} = \sigma_{\overline{R^t}}/\sigma_{R^t}$ at each receiver R is the argument of an inverse tangent function. At a given time t, if there is no coherent noise at one of the receivers, then no signal emerges from the correlation: $C_{AB}^{ob}(t) = 0$ because w_{R^t} tends to infinity so $1 - \frac{2}{\pi}\arctan(w_{R^t}) = 0$. On the contrary, if the coherent energy is large with respect to the incoherent energy at both receivers, then most of the n samples contribute to the correlation so $|C_{AB}^{ob}(t)|$ is large. As long as coherent and incoherent noise exist, eq. (52) is valid. In Section 3 we defined these two kinds of noise in the case of a uniform distribution of sources. One can reasonably think that they also exist in the case of other distributions.

4.2 The one-bit noise correlation in the case of a uniform distribution of sources

Now we study what (52) becomes in the case of a uniform distribution of noise sources. From eqs (29) and (30) we have

$$\sigma_{\overline{A^t}}^2 = \sigma_A^2 - \sigma_{A^t}^2, \tag{53}$$

$$\sigma_{\overline{B^t}}^2 = \sigma_B^2 - \sigma_{B^t}^2, \tag{54}$$

respectively, where σ_A^2 and σ_B^2 are the variance of $A(t)$ and $B(t)$, respectively. Then

$$|C_{AB}^{ob}(t)| = \left[1 - \frac{2}{\pi}\arctan\sqrt{\frac{\sigma_A^2}{\sigma_{A^t}^2} - 1}\right]\left[1 - \frac{2}{\pi}\arctan\sqrt{\frac{\sigma_B^2}{\sigma_{B^t}^2} - 1}\right]. \tag{55}$$

In this last expression, we normalized the correlation by the number of samples. The distribution of sources is uniform so $\sigma_A^2 = \sigma_B^2 = \sigma^2$, where $\sigma^2 = C_{UU}(t=0)$ is the autocorrelation peak at any point U at the surface of the medium. Moreover, eq. (48) (and also eqs 35 and 36 in the case of a large $\Delta\omega$) shows that

$$\sigma_{A^t}^2 = \sigma_{B^t}^2 = |C_{AB}(t)|, \tag{56}$$

so (55) becomes

$$|C_{AB}^{ob}(t)| = \left[1 - \frac{2}{\pi}\arctan\sqrt{\frac{\sigma^2}{|C_{AB}(t)|} - 1}\right]^2. \tag{57}$$

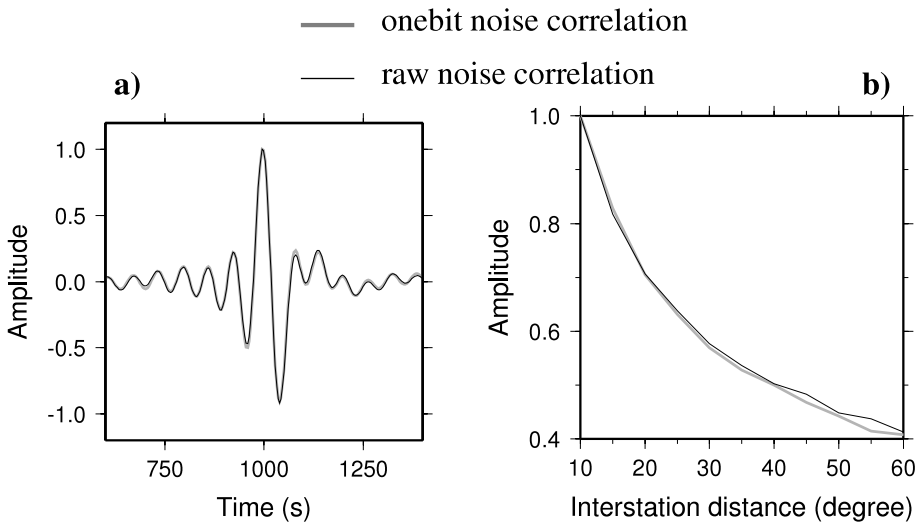

Figure 5. Comparison between raw noise correlations and one-bit noise correlations obtained by numerical simulation (*cf.* Fig. 1a). The time-derivatives of the two waveforms from the pair of stations 0 and 6 are very similar (a). The amplitude decays along the array of receivers also match very well (b).

Noting that $\sigma^2 \gg |C_{AB}(t)|$ and $\arctan \frac{1}{x} = \frac{\pi}{2} - \arctan x$, $\forall x \in \mathbb{R}^{+*}$, we obtain

$$|C_{AB}^{ob}(t)| = \left[\frac{2}{\pi} \arctan \sqrt{\frac{|C_{AB}(t)|}{\sigma^2}} \right]^2 . \tag{58}$$

The argument of the arctan function is close to zero so the first term of its Taylor series ($\arctan x = x$) can be used as a good linear approximation. It follows that

$$|C_{AB}^{ob}(t)| = \left(\frac{2}{\pi\sigma} \right)^2 |C_{AB}(t)|. \tag{59}$$

This equation sets the equality between the raw and the one-bit noise correlations in the case of a uniform distribution of noise sources generating fundamental mode surface waves. Of course, the absolute amplitudes are not the same but the waveforms and the relative amplitudes are identical. Previous works (Derode *et al.* 1999; Larose *et al.* 2004) showed the emergence of a signal from a one-bit noise correlation and studied its signal-to-noise ratio, but it is the first time that the equality (59) is demonstrated. Correlations from the numerical simulation (*cf.* Fig. 1a) illustrate our result. One-bit noise correlations are compared to raw noise correlations (Fig. 5). We see that the waveforms and the amplitude decays are the same.

5 WHAT HAPPENS IN AN ANELASTIC MEDIUM

We now introduce intrinsic attenuation in the medium. The fundamental mode Rayleigh wave GF between two points U and V then is

$$G_{UV}(\omega) = \frac{\exp\left[-\mathrm{i}\left(k\, d_{UV} + \frac{\pi}{4}\right)\right]}{\sqrt{\frac{\pi}{2}\, k\, d_{UV}}} \exp\left(-\frac{k\, d_{UV}}{2Q} \right), \tag{60}$$

where Q is the quality factor of the medium. Therefore, the raw noise correlation between $A(t)$ and $B(t)$ can be written in the frequency domain as

$$C_{AB}(\omega) = \frac{2}{\pi} \iint |S(\boldsymbol{r};\omega)|^2 \frac{\exp\left[\mathrm{i}\, k\, (d_A(\boldsymbol{r}) - d_B(\boldsymbol{r}))\right]}{k\sqrt{d_A(\boldsymbol{r})\, d_B(\boldsymbol{r})}} \exp\left[-\frac{k}{2Q} \left(d_A(\boldsymbol{r}) + d_B(\boldsymbol{r})\right) \right] \mathrm{d}\boldsymbol{r}. \tag{61}$$

We assume that $|S(\boldsymbol{r};\omega)|^2$ is a smooth function of $\boldsymbol{r}$ so we can use the stationary phase approximation. For the sake of simplicity, we consider the signal emerging from the sources at $x < 0$ only. We obtain

$$C_{AB}(\omega) = -\frac{2}{\mathrm{i}k} \frac{\exp\left[-\mathrm{i}\left(k\, \Delta + \frac{\pi}{4}\right)\right]}{\sqrt{\frac{\pi}{2}\, k\, \Delta}} \exp\left(-\frac{k\Delta}{2Q} \right) \int_{-\infty}^{0} |S(x, y = 0; \omega)|^2 \exp\left(\frac{kx}{Q} \right) \mathrm{d}x. \tag{62}$$

Expression (62) shows that the correlation contains the GF of the anelastic medium, including geometrical spreading as well as intrinsic attenuation. We assume a uniform distribution of noise so we get

$$C_{AB}(\omega) = -2L \frac{v(\omega)|S(\omega)|^2}{\mathrm{i}\omega} \frac{\exp\left[-\mathrm{i}\left(k\Delta + \frac{\pi}{4}\right)\right]}{\sqrt{\frac{\pi}{2} k \Delta}} \exp\left(-\frac{k\Delta}{2Q} \right), \tag{63}$$

where $L = \frac{Q}{k}$ is a factor also found by Snieder (2004). Eq. (63) shows that, again, the correlation has to be differentiate in time to match the GF. To check eq. (63), we carry out a new numerical experiment in which an anelastic PREM is considered. Results are shown in Fig. 6. We see that the time-derivative of the correlation fits both the waveform and the amplitude decay of the GF.

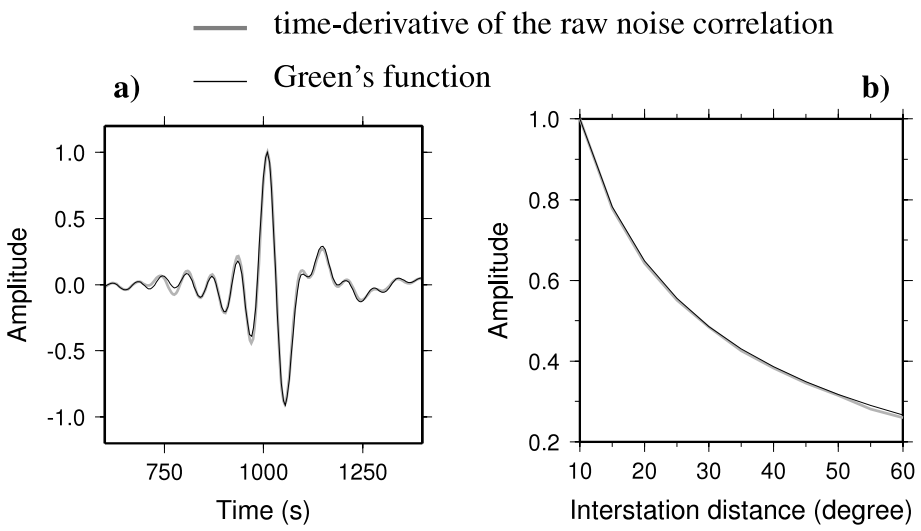

Figure 6. Comparison between the GF and the raw noise correlation in an anelastic earth. We use the pair of stations 0 and 6 to compare the waveforms (a). We see they are very similar. We also compare the amplitude decays (b). They are the same.

Following what we developed in Section 3, we introduce the functions $\sigma_A(\boldsymbol{r})$ and $\sigma_B(\boldsymbol{r})$ to write the correlation C_{AB} in the time domain as

$$C_{AB}(t) = \iint \sigma_A(\boldsymbol{r})\sigma_B(\boldsymbol{r})\rho_{AB}(\boldsymbol{r};t)\,\mathrm{d}\boldsymbol{r}. \tag{64}$$

In an anelastic medium, we have

$$\sigma_A(\boldsymbol{r}) = \frac{\exp\left(\frac{-k\,d_A(\boldsymbol{r})}{2Q}\right)}{\sqrt{d_A(\boldsymbol{r})}} \tag{65}$$

and

$$\sigma_B(\boldsymbol{r}) = \frac{\exp\left(\frac{-k\,d_B(\boldsymbol{r})}{2Q}\right)}{\sqrt{d_B(\boldsymbol{r})}}. \tag{66}$$

Using the inverse Fourier transform of eq. (61), we then find that the correlation coefficient ρ_{AB} is the same than in the pure elastic case (*cf.* eq. 17).

$$\rho_{AB}(\boldsymbol{r};t) = \frac{2}{\pi}\int \frac{|S(\boldsymbol{r};\omega)|^2}{k}\exp\left[\mathrm{i}\omega\left(t - \frac{d_B(\boldsymbol{r}) - d_A(\boldsymbol{r})}{v(\omega)}\right)\right]\mathrm{d}\omega. \tag{67}$$

The question now is to know if eq. (18) is still valid with the new definition of $\sigma_A(\boldsymbol{r})$ and $\sigma_B(\boldsymbol{r})$ (expressions 65 and 66). If so, then we will be able to define coherent and incoherent noise, and the general formula for the one-bit noise correlation (52) (and also 55) will be usable. Appendix D shows that

$$\begin{aligned}\Psi_A(t) &= \iint \sigma_A^2(\boldsymbol{r})\rho_{AB}(\boldsymbol{r},t)\,\mathrm{d}\boldsymbol{r}\\ &= -2\,\Delta\,\Gamma\left(\frac{1}{2}\right)\int \frac{v(\omega)|S(\omega)|^2}{\mathrm{i}\omega}\,U\left(\frac{1}{2},2;\frac{k\Delta}{Q}\right)\frac{\exp\left[\mathrm{i}\left(\omega t - k\Delta - \frac{\pi}{4}\right)\right]}{\sqrt{\frac{\pi}{2}k\Delta}}\mathrm{d}\omega\end{aligned} \tag{68}$$

and

$$\begin{aligned}\Psi_B(t) &= \iint \sigma_B^2(\boldsymbol{r})\rho_{AB}(\boldsymbol{r},t)\,\mathrm{d}\boldsymbol{r}\\ &= -2\,\Delta\,\Gamma\left(\frac{3}{2}\right)\int \frac{v(\omega)|S(\omega)|^2}{\mathrm{i}\omega}\,U\left(\frac{3}{2},2;\frac{k\Delta}{Q}\right)\frac{\exp\left[\mathrm{i}\left(\omega t - k\Delta - \frac{\pi}{4}\right)\right]}{\sqrt{\frac{\pi}{2}k\Delta}}\exp\left(-\frac{k\Delta}{Q}\right)\mathrm{d}\omega.\end{aligned} \tag{69}$$

Considering the real part of these equations and assuming that $v(\omega) = v$ and $|S(\omega)| = H(\omega_0 + \frac{\Delta\omega}{2}) - H(\omega_0 - \frac{\Delta\omega}{2})$, we get

$$\Psi_A(t) = 2\,\Delta\,v\,\Gamma\left(\frac{1}{2}\right)\int_{\omega_0-\frac{\Delta\omega}{2}}^{\omega_0+\frac{\Delta\omega}{2}} U\left(\frac{1}{2},2;\frac{k\Delta}{Q}\right)\frac{\cos\left(\omega t - k\Delta + \frac{\pi}{4}\right)}{\omega\sqrt{\frac{\pi}{2}k\Delta}}\,\mathrm{d}\omega \tag{70}$$

and

$$\Psi_B(t) = 2\,\Delta\,v\,\Gamma\left(\frac{3}{2}\right)\int_{\omega_0-\frac{\Delta\omega}{2}}^{\omega_0+\frac{\Delta\omega}{2}} U\left(\frac{3}{2},2;\frac{k\Delta}{Q}\right)\frac{\cos\left(\omega t - k\Delta + \frac{\pi}{4}\right)}{\omega\sqrt{\frac{\pi}{2}k\Delta}}\exp\left(-\frac{k\Delta}{Q}\right)\mathrm{d}\omega. \tag{71}$$

In Fig. 7, we plot the two normalized functions $\Psi_A(t)$ and $\Psi_B(t)$ for two different values of $\Delta\omega$ ($1.99\omega_0$ and ω_0) and two different values of Q (50 and 500). When Q is high, the two curves (plain blue for Ψ_A, red dashed for Ψ_B) are hardly distinguishable. This is not surprising: the intrinsic attenuation is small so we are close to the elastic case and we have $\Psi_A(t) \propto \Psi_B(t)$ (the absolute amplitudes are different so there is no equality). When Q is small, the effect of the intrinsic attenuation is significant and breaks the proportionality between the two functions. In the same figure, we also plot the product $\Psi_A(t)\Psi_B(t)$ and we compare the result with the square of the correlation (63) written in the time domain.

$$C_{AB}(t) = 2\,Q\,v^2 \int_{\omega_0-\frac{\Delta\omega}{2}}^{\omega_0+\frac{\Delta\omega}{2}} \frac{\cos\left(\omega t - k\Delta + \frac{\pi}{4}\right)}{\omega^2\sqrt{\frac{\pi}{2}k\Delta}} \exp\left(-\frac{k\Delta}{2Q}\right) \mathrm{d}\omega. \tag{72}$$

The two curves (plain blue for $\Psi_A(t)\Psi_B(t)$, red dashed for $C^2_{AB}(t)$) are normalized. In each case, they match very well. This is a nice result because it shows that eq. (18) still holds (up to a constant) in the anelastic case. We are not able to demonstrate this result analytically but the extreme values of Q (50 and 500 correspond to extremely low and high magnitudes in the Earth) and $\Delta\omega$ we use are good grounds to assess it, at least to first order. Finally, we plot $\Psi_A(t)\Psi_B(t)$ and $C^2_{AB}(t)$ at $t = t_0 = \frac{\Delta}{2} - \frac{\pi}{\omega_0 4}$ as a function of the interstation distance Δ ranging from $3\lambda_0$ to $20\lambda_0$. Again, the curves match very well. This means that the proportionality constant between $\Psi_A(t)\Psi_B(t)$ and $C^2_{AB}(t)$ is not a function of Δ. In other words, the amplitude decay of $\Psi_A(t)\Psi_B(t)$ is the same as the amplitude decay of $C^2_{AB}(t)$. We are now allowed to write

$$C^2_{AB}(t) \simeq \alpha\Psi_A(t)\Psi_B(t), \tag{73}$$

where α is a positive constant over t and Δ. As the expression of $\rho_{AB}(\boldsymbol{r};t)$ used in the definition of $\Psi_A(t)$ and $\Psi_B(t)$ is the same as the one in the elastic case (*cf.* eqs 17 and 67), we can take advantage of all the properties detailed in Section 3 and define coherent and incoherent noise. Therefore, formula (55) can be used to express the one-bit noise correlation. Putting the constant α into $\sigma^2_{A^t}$, we find

$$|C^{ob}_{AB}(t)| = \left[1 - \frac{2}{\pi}\arctan\sqrt{\frac{\sigma^2_A}{\alpha|\Psi_A(t)|} - 1}\right]\left[1 - \frac{2}{\pi}\arctan\sqrt{\frac{\sigma^2_B}{|\Psi_B(t)|} - 1}\right]. \tag{74}$$

The distribution of noise sources is uniform so, again, we can use the fact that $\sigma^2_A = \sigma^2_B = \sigma^2 = C_{UU}(t=0) \gg \Psi_{A,B}(t)$ to reduce (74) to

$$|C^{ob}_{AB}(t)| = \left(\frac{2}{\pi\sigma}\right)^2 \sqrt{\alpha|\Psi_A(t)|}\sqrt{|\Psi_B(t)|}. \tag{75}$$

$\Psi_A(t)$ and $\Psi_B(t)$ have same sign so (75) becomes

$$|C^{ob}_{AB}(t)| = \left(\frac{2}{\pi\sigma}\right)^2 \sqrt{\alpha\Psi_A(t)\Psi_B(t)} \tag{76}$$

$$\simeq \left(\frac{2}{\pi\sigma}\right)^2 |C_{AB}(t)|. \tag{77}$$

Similarly to the elastic case, we find that the one-bit noise correlation is equal to the raw noise correlation. This is confirmed by numerical results. In Fig. 8 we compare the waveforms and the amplitude decays of raw and one-bit noise correlations. We see they are the same.

6 DISCUSSION AND CONCLUSIONS

We provided an expression for the one-bit noise correlation. This expression involves the standard deviations of coherent and incoherent noise. For a given lag time t, the coherent noise $A^t(\tau)$ at a receiver A is a Gaussian signal that one can extract from the full noise record $A(\tau)$ and that perfectly correlates with the coherent noise $B^t(t+\tau)$ from another full noise record $B(t+\tau)$ at a receiver B. Then, the correlation of the coherent noises is exactly the correlation of the full noise records: $\int A(\tau)B(t+\tau)\mathrm{d}\tau = \int A^t(\tau)B^t(t+\tau)\mathrm{d}\tau$. The incoherent noise is the difference between the full noise record and the coherent noise. As long as you can define these two kinds of noise, our expression of the one-bit noise correlation is valid.

In this work, we detailed the coherent and incoherent standard deviations in the case of a uniform distribution of noise sources generating surface waves on a laterally homogeneous half-space. In this case, we showed that the one-bit noise correlation is equal to the raw noise correlation and so contains the GF. This property has been known for a long time. It is true in both elastic and anelastic media and it has been extensively used so far (e.g. Shapiro & Campillo 2004; Shapiro *et al.* 2005; Larose *et al.* 2007; Yao & van der Hilst 2009). Nevertheless, there was no theoretical proof of it. We here give one for the first time. An important result is that the equality does not only hold for the waveform but also for the relative amplitude: both geometrical spreading and intrinsic attenuation of the GF are retrieved by the one-bit noise correlation when the distribution of noise sources is uniform. This means that information can be extracted from the amplitude of one-bit noise correlations, which is not obvious because one-bit normalization is a very strong operation on the amplitude of noise recordings. In the case of a non-uniform distribution of sources, one has to study the coherent and incoherent standard deviations which correspond to the

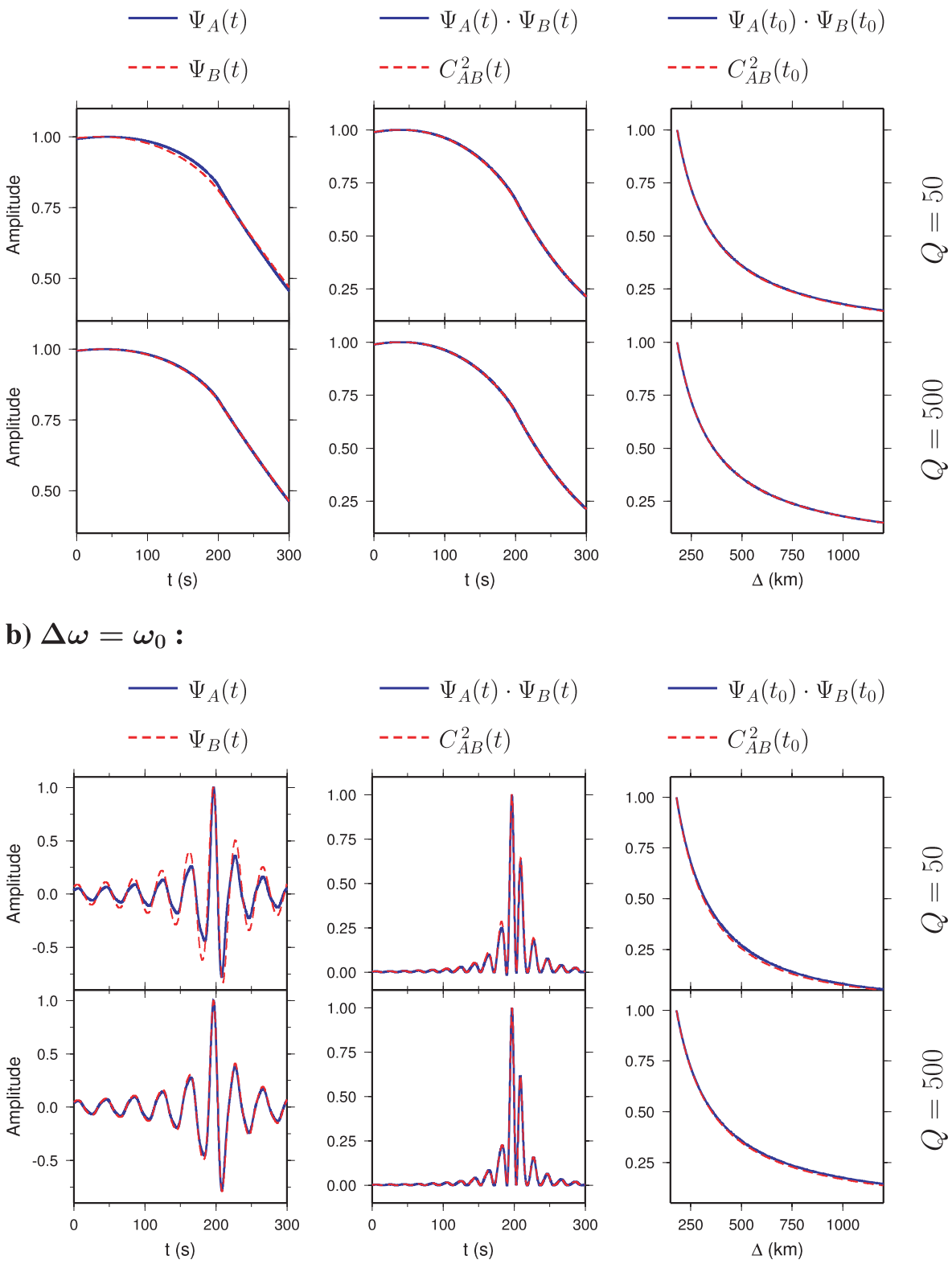

Figure 7. Comparison between $\Psi_A(t)$ and $\Psi_B(t)$ (left-hand side column), $\Psi_A(t)\Psi_B(t)$ and C^2_{AB} (t) (middle column) and $\Psi_A(t_0)\Psi_B(t_0)$ and C^2_{AB} (t_0) as a function of Δ (right-hand side column) for two different values of $\Delta\omega$: $1.99\,\omega_0$ (a) and ω_0 (b). The medium is anelastic. Two different values of Q are tested: 50 and 500. The other parameters are $f_0 = 0.05$ Hz and $v = 3\,\mathrm{km\,s^{-1}}$. All the waveforms (functions of t) are computed using $\Delta = 10\,\lambda_0 = 600$ km.

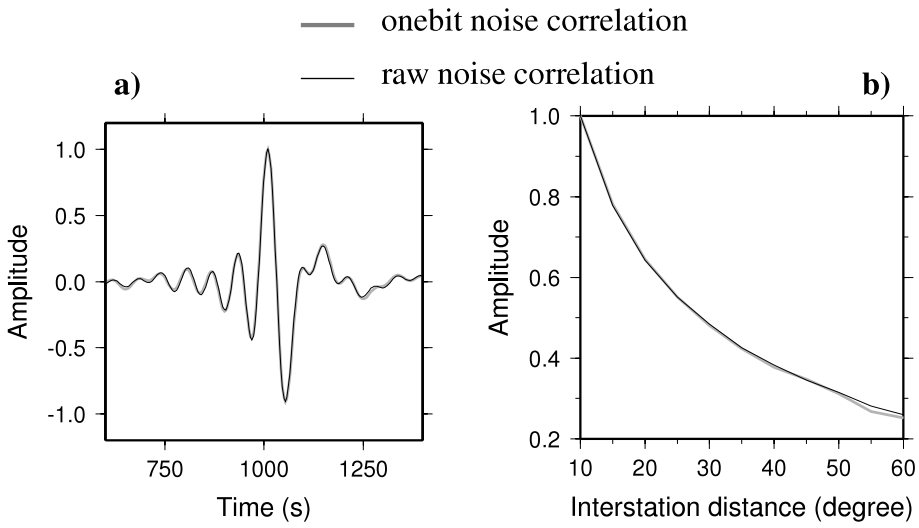

Figure 8. Same as Fig. 5 in an anelastic earth.

given distribution to estimate both the waveform and the relative amplitude of one-bit noise correlations. This is in agreement with numerical studies carried out by Cupillard & Capdeville (2010).

In pure elastic media, eq. (18) is rigorously demonstrated. This equation is at the basis of our theory. It relates the square of the raw noise correlation $C^2_{AB}(t)$ and the variances $\Psi_A(t)$ and $\Psi_B(t)$. In anelastic media, $C^2_{AB}(t)$ is plotted and compared with the product $\Psi_A(t) \times \Psi_B(t)$ to check if the expression is valid (Fig. 7, middle column) but no rigorous demonstration is provided. On the four plots, the curves are very similar but they are not exactly the same. It is particularly visible when $\Delta\omega = \omega_0$ and $Q = 50$. This means that eq. (18) is only true to first order when using the expressions we found for the coherent variances in the anelastic case. Further investigations are needed to check if exact expressions of the variances exist in this case. Here, we use approximate expressions and we assume that the small discrepancies in the amplitude decays (Fig. 7, right-hand side column) are due to these approximations. If it is not the case (i.e. if the small discrepancies are effective in practice), then measurements of intrinsic attenuation from one-bit noise correlations will give approximate values of Q.

The derivation shown in this paper involves surface waves. It should be easy to write it for body waves as well. The GF between two points U and V would be

$$G_{UV}(\omega) = \frac{\exp(-\mathrm{i}kd_{UV})}{d_{UV}}, \tag{78}$$

and the coherent noise could be defined using the following correlation coefficient:

$$\rho_{AB}(\theta;t) = \int_{\omega_0-\frac{\Delta\omega}{2}}^{\omega_0+\frac{\Delta\omega}{2}} \cos\left[\omega\left(t+\frac{\Delta\sin\theta}{v}\right)\right]\mathrm{d}\omega \tag{79}$$

$$= \Delta\omega\,\mathrm{sinc}\left[\frac{\Delta\omega}{2}\left(t+\frac{\Delta\sin\theta}{v}\right)\right]\cos\left[\omega_0\left(t+\frac{\Delta\sin\theta}{v}\right)\right]. \tag{80}$$

This last expression is very similar to the correlation coefficient introduced in the review paper by Larose (2006). This means that our definition of coherency is actually the same as previous definitions (Snieder 2004; Roux *et al.* 2005; Sabra *et al.* 2005). Here, we just go into the details of the concept to extract the properties we need to understand the one-bit noise correlation.

The analytical expressions of the standard deviations we provide in this work are obtained in the case of a 1-D layered medium. An extension of these expressions to a full 3-D case is not straightforward. It would require a description of complex GFs, and scattering should be taken into account (Halliday & Curtis 2009). Scatterers act as secondary noise sources and drastically change the size of the coherent and incoherent hyperbolas. When dealing with coda recordings, these hyperbolas depend on the part of the coda that is in use because such recordings are non-stationary. In this case, our statistical model would need standard deviations which depend on the time in the noise record, as suggested by Derode *et al.* (1999) and Larose *et al.* (2008). To study full 3-D cases, numerical simulations are actually necessary. Using numerical tools to evaluate standard deviations and understand what the one-bit noise correlation exactly contains in complex media will be the topic of future work.

ACKNOWLEDGMENTS

The authors would like to thank Francisco J. Sánchez-Sesma, Vedran Lekic, Yann Capdeville, Eric Larose and Michel Campillo for valuable discussions. Constructive comments from two anonymous reviewers and editor David Halliday also helped to improve the manuscript. This work was partially supported by NSF grant EAR-0738284. This is Berkeley Seismological Laboratory contribution 10-14.

REFERENCES

Abramowitz, M. & Stegun, I.A., 1972. *Handbook of Mathematical Functions with Formulas, Graphs, and Mathematical Tables*, 9th printing, Dover, New York.

Aki, K. & Richards, P.G., 2002. *Quantitative Seismology*, 2nd edn, University Science Books, Sausalito.

Bensen, G.D., Ritzwoller, M.H., Barmin, M.P., Levshin, A.L., Lin, F., Moschetti, M.P., Shapiro, N.M. & Yang, Y., 2007. Processing seismic ambient noise data to obtain reliable broad-band surface wave dispersion measurements, *Geophys. J. Int.*, **169**, 1239–1260, doi:10.1111/j.1365–246X.2007.03374.x.

Bensen, G.D., Ritzwoller, M.H., Barmin, M.P., Levshin, A.L., Lin, F., Moschetti, M.P., Shapiro, N.M. & Yang, Y., 2008. Broad-band ambient noise surface wave tomography across the united states, *J. geophys. Res.*, **113**, B05306, doi:10.1029/2007JB005248.

Bond, F.E. & Cahn, C.R., 1958. On sampling the zeros of bandwidth limited signals. *IRE Trans. Inform. Theory*, **4**, 110–113.

Brooks, L. & Gerstoft, P., 2009. Green's function approximation from cross-correlations of 20–100 Hz noise during a tropical storm, *J. acoust. Soc. Am.*, **125**(2), 723–734.

Campillo, M. & Paul, A., 2003. Long-range correlations in the diffuse seismic coda, *Science*, **299**, 547–549.

Cho, K., Herrmann, R.B., Ammon, C.J. & Lee, K., 2007. Imaging the upper crust of the korean peninsula by surface-wave tomography, *Bull. seism. Soc. Am.*, **67**, 198–207.

Cupillard, P. & Capdeville, Y., 2010. On the amplitude of surface waves obtained by noise correlation and the capability to recover the attenuation: a numerical approach, *Geophys. J. Int.*, **181**(3), 1687–1700, doi:10.1111/j.1365–246X.2010.04586.x.

Derode, A., Tourin, A. & Fink, M., 1999. Ultrasonic pulse compression with one-bit time reversal through multiple scattering, *J. appl. Phys.*, **85**, 6343–6352.

Derode, A., Larose, E., Tanter, M., de Rosny, J., Tourin, A., Campillo, M. & Fink, M., 2003. Recovering the Green's function from field-field correlations in an open scattering medium (L), *J. acoust. Soc. Am.*, **113**, 2973–2976.

Dziewonski, A.M. & Anderson, D.L., 1981. Preliminary reference Earth model. *Phys. Earth planet. Inter.*, **25**, 297–356.

Friedrich, A., Krüger, F. & Klinge, K., 1998. Ocean-generated microseismic noise located with the Gräfenberg array, *J. Seismol.*, **2**, 47–64.

Gerstoft, P. & Tanimoto, T., 2007. A year of microseisms in southern California, *Geophys. Res. Lett.*, **34**, L20304, doi:10.1029/2007GL031091.

Gradshteyn, I.S. & Ryzhik, I.M., 2007. *Table of Integrals, Series and Products*, 7th edn, eds Jeffrey, A. & Zwillinger, D., Academic Press, Burlington.

Halliday, D. & Curtis, A., 2008. Seismic interferometry, surface waves and source distribution, *Geophys. J. Int.*, **175**, 1067–1087, doi:10.1111/j.1365–246X.2008.03918.x.

Halliday, D. & Curtis, A., 2009. Seismic interferometry of scattered surface waves in attenuative media, *Geophys. J. Int.*, **178**, 419–446, doi:10.1111/j.1365–246X.2009.04153.x.

Kedar, S., Longuet-Higgins, M., Webb, F., Graham, N., Clayton, R. & Jones, C., 2008. The origin of deep ocean microseisms in the North Atlantic Ocean, *Proc. R. Soc. A*, **464**, 777–793.

Kimman, W.P. & Trampert, J., 2010. Approximations in seismic interferometry and their effects on surface waves, *Geophys. J. Int.*, **182**, 461–476, doi:10.1111/j.1365–246X.2010.04632.x.

Larose, E., 2006. Mesoscopics of ultrasound and seismic waves: application to passive imaging, *Ann. Phys. Fr.*, **31**(3), 1–126, doi:10.1051/anphys:2007001.

Larose, E., Derode, A., Campillo, M. & Fink, M., 2004. Imaging from one-bit correlations of wide-band diffuse wavefields, *J. appl. Phys.*, **95**(12), 8393–8399.

Larose, E., Roux, P. & Campillo, M., 2007. Reconstruction of Rayleigh-Lamb dispersion spectrum based on noise obtained from an air-jet forcing, *J. acoust. Soc. Am.*, **122**(6), 3437–3444.

Larose, E., Roux, P., Campillo, M. & Derode, A., 2008. Fluctuations of correlations and Green's function reconstruction: role of scattering, *J. appl. Phys.*, **103**, 114907, doi:10.1063/1.2939267.

Lin, F., Ritzwoller, M.H., Townend, J., Savage, M. & Bannister, S., 2007. Ambient noise Rayleigh wave tomography of New Zealand, *Geophys. J. Int.*, **170**, 649–666, doi:10.1111/j.1365–246X.2007.03414.x.

Lin, F., Moschetti, M.P. & Ritzwoller, M.H., 2008. Surface wave tomography of the western United States from ambient seismic noise: Rayleigh and Love wave phase velocity maps, *Geophys. J. Int.*, **173**, 281–298, doi:10.1111/j1365–246X.2008.03720.x.

Lobkis, O.I. & Weaver, R.L., 2001. On the emergence of the Green's function in the correlation of a diffuse field, *J. acoust. Soc. Am.*, **110**, 3011–3017.

Longuet-Higgins, M.S., 1950. A theory on the origin of microseisms, *Phil. Trans. R. Soc. Lond. A.*, **243**, 1–35.

Matzel, E., 2008. Attenuation tomography using ambient noise correlation, *Seism. Res. Lett.*, **79**(2), 358.

Pedersen, H.A., Krüger, F. & the SVEKALAPKO Seismic Tomography Working Group, 2007. Inłuence of the seismic noise characteristics on noise correlations in the Baltic shield, *Geophys. J. Int.*, **168**, 197–210, doi:10.1111/j.1365–246X.2006.03177.x.

Prieto, G.A., Lawrence, J.F. & Beroza, G.C., 2009. Anelastic Earth structure from the coherency of the ambient seismic field, *J. geophys. Res.*, **144**, B07303, doi:10.1029/2008JB006067.

Roux, P., Sabra, K.G. & Kuperman, W.A., 2005. Ambient noise cross-correlation in free space: theoretical approach, *J. acoust. Soc. Am.*, **117**(1), 79–84, doi:10.1121/1.1830673.

Sabra, K.G., Roux, P. & Kuperman, W.A., 2005. Arrival-time structure of the time-averaged ambient noise cross-correlation function in an oceanic waveguide, *J. acoust. Soc. Am.*, **117**(1), 164–174, doi:10.1121/1.1835507.

Schulte-Pelkum, V., Earle, P.S. & Vernon, F.L., 2004. Strong directivity of ocean-generated seismic noise, *Geochem. Geophys. Geosyst.*, **5**, Q03004, doi:10.1029/2003GC000520.

Shapiro, N.M. & Campillo, M., 2004. Emergence of broadband Rayleigh waves from correlations of the ambient seismic noise, *Geophys. Res. Lett.*, **31**, L07614, doi:10.1029/2004GL019491.

Shapiro, N.M., Campillo, M., Stehly, L. & Ritzwoller, M.H., 2005. High-resolution surface wave tomography from ambient seismic noise, *Science*, **307**, 1615–1618.

Snieder, R., 2004. Extracting the Green's function from the correlation of coda waves: a derivation based on stationary phase, *Phys. Rev. E*, **69**, 046610, doi:10.1103/PhysRevE.69.046610.

Stehly, L., Campillo, M. & Shapiro, N., 2006. A study of the seismic noise from its long-range correlation properties, *J. geophys. Res.*, **111**, B10306, doi:10.1029/2005JB004237.

Stehly, L., Fry, B., Campillo, M., Shapiro, N., Guilbert, J., Boschi, L. & Giardini, D., 2009. Tomography of the alpine region from observations of seismic ambient noise, *Geophys. J. Int.*, **178**, 338–350, doi:10.1111/j.1365–246X.2009.04132.x.

Stutzmann, E., Schimmel, M., Patau, G. & Maggi, A., 2009. Global climate imprint on seismic noise, *Geochem. Geophys. Geosyst.*, **10**, Q11004, doi:10.1029/2009GC002619.

van Tiggelen, B.A., 2003. Green function retrieval and time-reversal in a disordered world, *Phys. Rev. Lett.*, **91**(24), 243904, doi:10.1103/PhysRevLett.91.243904.

Voelcker, H.B., 1966a. Toward a unified theory of modulation. Part I: phase-envelope relationships, *Proc. IEEE*, **54**(3), 340–353.

Voelcker, H.B., 1966b. Toward a unified theory of modulation. Part II: zero manipulation, *Proc. IEEE*, **54**(5), 735–755.

Voelcker, H.B. & Requicha, A.A.G., 1973. Clipping and signal determinism: two algorithms requiring validation, *IEEE Trans. Commun.*, COM-21(6), 738–744.

Wapenaar, K., 2004. Retrieving the elastodynamic Green's function of an arbitrary inhomogeneous medium by cross-correlation, *Phys. Rev. Lett.*, **93**, 254–301, doi:10.1103/PhysRevLett.93.254301.

Woodhouse, J.H. & Girnius, T.P., 1982. Surface waves and free oscillations in a regionalized earth model, *Geophys. J. R. astr. Soc.*, **78**, 641–660.

Yang, Y. & Ritzwoller, M.H., 2008. Characteristics of ambient seismic noise as a source for surface wave tomography, *Geochem. Geophys. Geosyst.*, **9**, Q02008, doi:10.1029/2007GC001814.

Yang, Y., Ritzwoller, M.H., Levshin, A.L. & Shapiro, N.M., 2007. Ambient noise Rayleigh wave tomography across Europe, *Geophys. J. Int.*, **168**, 259–274.

Yao, H. & van der Hilst, R.D., 2009. Analysis of ambient noise energy distribution and phase velocity bias in ambient noise tomography, with application to SE Tibet, *Geophys. J. Int.*, **179**, 1113–1132.

Yao, H., van der Hilst, R.D. & de Hoop, M.V., 2006. Surface-wave array tomography in SE Tibet from ambient seismic noise and two-station analysis, I: phase velocity maps, *Geophys. J. Int.*, **166**, 732–744, doi:10.1111/j.1365–246X.2006.03028.x.

Yao, H., van der Hilst, R.D. & de Hoop, M.V., 2008. Surface-wave array tomography in SE Tibet from ambient seismic noise and two-station analysis, II: crustal and upper-mantle structure, *Geophys. J. Int.*, **173**, 205–219, doi:10.1111/j.1365–246X.2007.03696.x.

APPENDIX A: PROOF OF EXPRESSION (18)

The goal of this appendix is to demonstrate that, in the case of a uniform distribution of noise sources, we have

$$\Psi_A(t)\Psi_B(t) = C_{AB}^2(t), \tag{A1}$$

with

$$\Psi_A(t) = \iint \sigma_A^2(\boldsymbol{r})\rho_{AB}(\boldsymbol{r}, t)\,\mathrm{d}\boldsymbol{r} \tag{A2}$$

and

$$\Psi_B(t) = \iint \sigma_B^2(\boldsymbol{r})\rho_{AB}(\boldsymbol{r}, t)\,\mathrm{d}\boldsymbol{r}. \tag{A3}$$

We start from the Fourier transform of $\Psi_A(t)$:

$$\Psi_A(\omega) = \frac{2}{\pi k}\iint \frac{|S(\boldsymbol{r};\omega)|^2}{d_A(\boldsymbol{r})}\exp\left[\mathrm{i}\,k\,(d_A(\boldsymbol{r}) - d_B(\boldsymbol{r}))\right]\mathrm{d}\boldsymbol{r}. \tag{A4}$$

When $|S(\boldsymbol{r};\omega)|^2$ is a smooth function of $\boldsymbol{r}$, this integral can be evaluated using the stationary phase approximation:

$$\begin{aligned}\Psi_A(\omega) = {} & \frac{2}{\mathrm{i}k}\frac{\exp\left[\mathrm{i}\left(k\Delta + \frac{\pi}{4}\right)\right]}{\sqrt{\frac{\pi}{2}k\Delta}}\int_\Delta^\infty |S(x, y=0;\omega)|^2\sqrt{\frac{x-\Delta}{x}}\,\mathrm{d}x \\ & - \frac{2}{\mathrm{i}k}\frac{\exp\left[-\mathrm{i}\left(k\Delta + \frac{\pi}{4}\right)\right]}{\sqrt{\frac{\pi}{2}k\Delta}}\int_{-\infty}^0 |S(x, y=0;\omega)|^2\sqrt{\frac{x-\Delta}{x}}\,\mathrm{d}x.\end{aligned} \tag{A5}$$

Assuming a uniform distribution of noise sources ($|S(x, y=0;\omega)|^2 = |S(\omega)|^2$), it follows that

$$\begin{aligned}\Psi_A(\omega) = {} & 2D\frac{v(\omega)|S(\omega)|^2}{\mathrm{i}\omega}\frac{\exp\left[\mathrm{i}\left(k\Delta + \frac{\pi}{4}\right)\right]}{\sqrt{\frac{\pi}{2}k\Delta}}\left[1 - \frac{\Delta}{2D}\ln\left(\frac{4D}{\Delta}\right) + o\left(\frac{\Delta}{D}\right)\right] \\ & - 2D\frac{v(\omega)|S(\omega)|^2}{\mathrm{i}\omega}\frac{\exp\left[-\mathrm{i}\left(k\Delta + \frac{\pi}{4}\right)\right]}{\sqrt{\frac{\pi}{2}k\Delta}}\left[1 + \frac{\Delta}{2D}\ln\left(\frac{4D}{\Delta}\right) + o\left(\frac{\Delta}{D}\right)\right],\end{aligned} \tag{A6}$$

where $D \gg \Delta$ is a distance we introduce to perform the integration over x and prevent this integration to diverge.

In the same way we find

$$\begin{aligned}\Psi_B(\omega) = {} & \frac{2}{\mathrm{i}k}\frac{\exp\left[\mathrm{i}\left(k\Delta + \frac{\pi}{4}\right)\right]}{\sqrt{\frac{\pi}{2}k\Delta}}\int_\Delta^\infty |S(x, y=0;\omega)|^2\sqrt{\frac{x}{x-\Delta}}\,\mathrm{d}x \\ & - \frac{2}{\mathrm{i}k}\frac{\exp\left[-\mathrm{i}\left(k\Delta + \frac{\pi}{4}\right)\right]}{\sqrt{\frac{\pi}{2}k\Delta}}\int_{-\infty}^0 |S(x, y=0;\omega)|^2\sqrt{\frac{x}{x-\Delta}}\,\mathrm{d}x\end{aligned} \tag{A7}$$

$$\begin{aligned}= {} & 2D\frac{v(\omega)|S(\omega)|^2}{\mathrm{i}\omega}\frac{\exp\left[\mathrm{i}\left(k\Delta + \frac{\pi}{4}\right)\right]}{\sqrt{\frac{\pi}{2}k\Delta}}\left[1 + \frac{\Delta}{2D}\ln\left(\frac{4D}{\Delta}\right) + o\left(\frac{\Delta}{D}\right)\right] \\ & - 2D\frac{v(\omega)|S(\omega)|^2}{\mathrm{i}\omega}\frac{\exp\left[-\mathrm{i}\left(k\Delta + \frac{\pi}{4}\right)\right]}{\sqrt{\frac{\pi}{2}k\Delta}}\left[1 - \frac{\Delta}{2D}\ln\left(\frac{4D}{\Delta}\right) + o\left(\frac{\Delta}{D}\right)\right].\end{aligned} \tag{A8}$$

Writing (A6) and (A8) in the time domain, we finally get

$$\Psi_A(t)\Psi_B(t) = 4D^2\left\{\int \frac{v(\omega)|S(\omega)|^2}{\mathrm{i}\omega}\left[\frac{\exp\left[\mathrm{i}\left(k\Delta + \frac{\pi}{4}\right)\right]}{\sqrt{\frac{\pi}{2}k\Delta}} - \frac{\exp\left[-\mathrm{i}\left(k\Delta + \frac{\pi}{4}\right)\right]}{\sqrt{\frac{\pi}{2}k\Delta}}\right]\mathrm{e}^{\mathrm{i}\omega t}\,\mathrm{d}\omega\right\}^2\left[1 + o\left(\frac{\Delta}{D}\right)\right]. \tag{A9}$$

We recognize the first term on the right-hand side to be the square of the inverse Fourier transform of eq. (9), that is to say the square of the correlation between $A(t)$ and $B(t)$.

APPENDIX B: PRECISIONS ON EQ. (27)

The cosine-integral special function ci is defined in $\mathbb{R}^{+*}$ by (Abramowitz & Stegun 1972).

$$\mathrm{ci}(u) = -\int_u^{\infty} \frac{\cos x}{x}\mathrm{d}x. \tag{B1}$$

The extension of the definition of ci to $\mathbb{R}^{-*}$ is straightforward. Indeed, the change of variable $y = -x$ in eq. (B1) yields

$$\mathrm{ci}(u) = -\int_{-u}^{-\infty} \frac{\cos y}{y}\mathrm{d}y, \tag{B2}$$

so it is natural to pose $\mathrm{ci}(u) = \mathrm{ci}(-u)\ \forall u \in \mathbb{R}^{-*}$.

To fully describe expression (27), we now have to define the function $\mathrm{ci}[(\omega_0 + \frac{\Delta\omega}{2})(t+\alpha)] - \mathrm{ci}[(\omega_0 - \frac{\Delta\omega}{2})(t+\alpha)]$ in 0. To do so, we evaluate the limit of this function when $t \to -\alpha$. By definition we have

$$\mathrm{ci}\left[\left(\omega_0 + \frac{\Delta\omega}{2}\right)(t+\alpha)\right] - \mathrm{ci}\left[\left(\omega_0 - \frac{\Delta\omega}{2}\right)(t+\alpha)\right] = \int_{\omega_0-\frac{\Delta\omega}{2}}^{\omega_0+\frac{\Delta\omega}{2}} \frac{\cos[\omega(t+\alpha)]}{\omega}\mathrm{d}\omega, \tag{B3}$$

so

$$\lim_{t\to-\alpha} \mathrm{ci}\left[\left(\omega_0 + \frac{\Delta\omega}{2}\right)(t+\alpha)\right] - \mathrm{ci}\left[\left(\omega_0 - \frac{\Delta\omega}{2}\right)(t+\alpha)\right] = \lim_{t\to-\alpha}\int_{\omega_0-\frac{\Delta\omega}{2}}^{\omega_0+\frac{\Delta\omega}{2}} \frac{\mathrm{d}\omega}{\omega} \tag{B4}$$

$$= \ln\left(\frac{\omega_0 + \frac{\Delta\omega}{2}}{\omega_0 - \frac{\Delta\omega}{2}}\right). \tag{B5}$$

The limit exists and is finite, so eq. (27) is defined and continuous in 0.

APPENDIX C: PROOF OF EQ. (52)

The probability density function of the random variables $A^t(\tau)$ and $\overline{A^t}(\tau)$ is

$$f(x) = \frac{1}{\sigma_{A^t}\sqrt{2\pi}} \exp\left(\frac{-x^2}{2\,\sigma_{A^t}^2}\right) \tag{C1}$$

and

$$g(x) = \frac{1}{\sigma_{\overline{A^t}}\sqrt{2\pi}} \exp\left(\frac{-x^2}{2\,\sigma_{\overline{A^t}}^2}\right), \tag{C2}$$

respectively.

P_A^t is the probability that $|A^t(\tau)| > |\overline{A^t}(\tau)|$ so

$$P_A^t = \int_0^{\infty} 2g(x)\int_x^{\infty} 2f(y)\,\mathrm{d}y\,\mathrm{d}x \tag{C3}$$

$$= 1 - \frac{2}{\sqrt{\pi}}\int_0^{\infty} \mathrm{e}^{-x^2}\,\mathrm{erf}\left(\frac{\sigma_{\overline{A^t}}}{\sigma_{A^t}}x\right)\mathrm{d}x. \tag{C4}$$

This last integral can be calculated following Gradshteyn & Ryzhik (2007). Then

$$P_A^t = 1 - \frac{2}{\pi}\arctan\left(\frac{\sigma_{\overline{A^t}}}{\sigma_{A^t}}\right). \tag{C5}$$

In the same way we find the probability that $|B^t(\tau)| > |\overline{B^t}(\tau)|$:

$$P_B^t = 1 - \frac{2}{\pi}\arctan\left(\frac{\sigma_{\overline{B^t}}}{\sigma_{B^t}}\right). \tag{C6}$$

Finally, we obtain

$$|C_{AB}^{ob}(t)| = n\left[1 - \frac{2}{\pi}\arctan\left(\frac{\sigma_{\overline{A^t}}}{\sigma_{A^t}}\right)\right]\left[1 - \frac{2}{\pi}\arctan\left(\frac{\sigma_{\overline{B^t}}}{\sigma_{B^t}}\right)\right]. \tag{C7}$$

APPENDIX D: Ψ_A AND Ψ_B IN THE ANELASTIC CASE

$$\Psi_A(\omega) = \frac{2}{\pi k}\iint \frac{|S(\boldsymbol{r};\omega)|^2 \exp\left(\frac{-k\,d_A(\boldsymbol{r})}{Q}\right)}{d_A(\boldsymbol{r})} \exp\left[\mathrm{i}\,k\,(d_A(\boldsymbol{r}) - d_B(\boldsymbol{r}))\right]\mathrm{d}\boldsymbol{r}. \tag{D1}$$

Using the stationary phase approximation in the Cartesian coordinate system shown in Fig. 2, we can reduce this expression to

$$\Psi_A(\omega) = -\frac{2}{\mathrm{i}k}\frac{\exp\left[-\mathrm{i}\left(k\Delta+\frac{\pi}{4}\right)\right]}{\sqrt{\frac{\pi}{2}k\Delta}}\int_{-\infty}^{0}|S(x,y=0;\omega)|^2\exp\left(\frac{kx}{Q}\right)\sqrt{\frac{x-\Delta}{x}}\,\mathrm{d}x. \tag{D2}$$

To get this expression, we considered the signal emerging from the sources at $x < 0$ only. Assuming a uniform distribution of noise sources ($|S(x, y = 0;\omega)|^2 = |S(\omega)|^2$), we are able to perform the integral over x following Gradshteyn & Ryzhik (2007). Expression (D2) then becomes

$$\Psi_A(\omega) = -\frac{2\Delta}{\mathrm{i}k}\,\Gamma\left(\frac{1}{2}\right)|S(\omega)|^2\,U\left(\frac{1}{2},2;\frac{k\Delta}{Q}\right)\frac{\exp\left[-\mathrm{i}\left(k\Delta+\frac{\pi}{4}\right)\right]}{\sqrt{\frac{\pi}{2}k\Delta}}, \tag{D3}$$

where Γ is the gamma function and U is the confluent hypergeometric function of the second kind (Abramowitz & Stegun 1972). Writing eq. (D3) in the time domain, we get

$$\Psi_A(t) = -2\,\Delta\,\Gamma\left(\frac{1}{2}\right)\int\frac{|S(\omega)|^2}{\mathrm{i}k}\,U\left(\frac{1}{2},2;\frac{k\Delta}{Q}\right)\frac{\exp\left[\mathrm{i}\left(\omega t-k\Delta-\frac{\pi}{4}\right)\right]}{\sqrt{\frac{\pi}{2}k\Delta}}\mathrm{d}\omega. \tag{D4}$$

In the same way we find

$$\Psi_B(t) = -2\,\Delta\,\Gamma\left(\frac{3}{2}\right)\int\frac{|S(\omega)|^2}{\mathrm{i}k}\,U\left(\frac{3}{2},2;\frac{k\Delta}{Q}\right)\frac{\exp\left[\mathrm{i}\left(\omega t-k\Delta-\frac{\pi}{4}\right)\right]}{\sqrt{\frac{\pi}{2}k\Delta}}\exp\left(-\frac{k\Delta}{Q}\right)\mathrm{d}\omega. \tag{D5}$$